
Water Extract of Desalted *Salicornia europaea* Inhibits RANKL-induced Osteoclast Differentiation and Prevents Bone Loss in Ovariectomized Mice

Ah-Ra Jang , Yun-Ji Lee , Dong-Yeon Kim , Tae-Sung Lee , Do-Hyeon Jung , Yeong-Jun Kim , In-Su Seo , [Jae-Hun Ahn](#) , Eun-Jung Song , [Jisu Oh](#) , Aoding Li , Si Hoon Song , [Hyung-Sik Kim](#) , Min-Jung Kang , [Yoojin Seo](#) , [Jeong-Yong Cho](#) * , [Jong-Hwan Park](#) *

Posted Date: 6 November 2023

doi: 10.20944/preprints202311.0318.v1

Keywords: *Salicornia europaea*; Dicafeoylquinic acids; Bone loss; Osteoclast; Reactive oxygen



Preprints.org is a free multidiscipline platform providing preprint service that is dedicated to making early versions of research outputs permanently available and citable. Preprints posted at Preprints.org appear in Web of Science, Crossref, Google Scholar, Scilit, Europe PMC.

Copyright: This is an open access article distributed under the Creative Commons Attribution License which permits unrestricted use, distribution, and reproduction in any medium, provided the original work is properly cited.

Article

Water Extract of Desalted *Salicornia Europaea* Inhibits RANKL-Induced Osteoclast Differentiation and Prevents Bone Loss in Ovariectomized Mice

Ah-Ra Jang ^{1,2,†}, Yun-Ji Lee ^{1,†}, Dong-Yeon Kim ¹, Tae-Sung Lee ¹, Do-Hyeon Jung ¹, Yeong-Jun Kim ¹, In-Su Seo ¹, Jae-Hun Ahn ¹, Eun-Jung Song ², Jisu Oh ^{2,3}, Aoding Li ³, Si Hoon Song ³, Hyung-Sik Kim ^{4,5,6}, Min-Jung Kang ⁴, Yoojin Seo ⁴, Jeong-Yong Cho ^{3,*} and Jong-Hwan Park ^{1,2,*}

¹ Laboratory Animal Medicine, College of Veterinary Medicine and Animal Medical Institute, Chonnam National University, Gwangju 61186, Republic of Korea

² NODCURE, INC., 77 Yongbong-ro, Buk-gu, Gwangju 61186, Republic of Korea

³ Department of Food Science & Technology, Chonnam National University, Gwangju 61186 Republic of Korea

⁴ Department of Oral Biochemistry, Dental and Life Science Institute, School of Dentistry, Pusan National University, Yangsan 50612, Republic of Korea

⁵ Department of Life Science in Dentistry, School of Dentistry, Pusan National University, Yangsan 50612, Republic of Korea

⁶ Education and Research Team for Life Science on Dentistry, Pusan National University, Yangsan 50612, Republic of Korea

* Correspondence: jonpark@jnu.ac.kr

† These two authors equally contributed to this work.

Abstract: Osteoporosis, often linked to increased osteoclast activity due to menopause or aging, was the focus. In this study, the inhibitory effects of *Salicornia europaea* L. (SE) water extract of desalted SE (WSE) were investigated on osteoclast differentiation and bone loss in ovariectomized mice. The findings revealed that WSE effectively inhibited RANKL-induced osteoclast differentiation, as evidenced by TRAP staining, and also suppressed bone resorption and F-actin ring formation in a dose-dependent manner. Gene expressions related to osteoclast differentiation, including NFATc1, TRAP, cathepsin K, and DC-STAMP, were downregulated by WSE. Oral administration of WSE improved bone density and structural parameters in ovariectomized mice. Dicafeoyl quinic acids (DCQAs) and saponins in WSE were detected, with 3,4-, 3,5-, and 4,5-DCQA isolated and identified. All tested DCQAs, including the aforementioned types, inhibited osteoclast differentiation, bone resorption, and the expression of osteoclast-related genes. Furthermore, WSE and DCQAs reduced ROS production mediated by RANKL. These results indicate the potential of WSE and its components, DCQA, as preventive or therapeutic agents against osteoporosis and related conditions.

Keywords: salicornia europaea; dicafeoylquinic acids; bone loss; osteoclast; reactive oxygen

1. Introduction

The process of bone remodeling consists of the resorption of bone by osteoclasts and the formation of bone by osteoblasts, respectively. Homeostasis between these cells is crucial for maintaining bone mass and mineral metabolism. An imbalance between bone resorption of osteoclast and bone formation of osteoblast can lead to bone-related conditions, including osteoporosis and rheumatoid arthritis[1]. In older women, postmenopausal osteoporosis is a common metabolic bone disorder and is associated with decreased hormone levels[2]. Estrogen deficiency causes osteoclastic bone resorption and bone loss, leading to osteoporosis [3]. Hence, inhibition of osteoclast differentiation is considered the main therapeutic approach to osteoporosis.

Osteoclasts, which develop in the mononuclear cell/macrophage hematopoietic lineage, exhibit a multinucleated morphology. Osteoclast differentiation and activity are dependent on two essential

cytokines: receptor activator of nuclear factor-kappa B (NF- κ B) ligand (RANKL), a differentiation factor, and macrophage-colony stimulating factor (M-CSF), a survival factor [4]. RANKL-RANK binding leads to the recruitment of TNF receptor-associated factor 6 (TRAF6), which results in the activation of downstream signaling factors, such as NF- κ B and mitogen-activated protein kinases (MAPKs). Subsequently, nuclear factor of activated T cells c1 (NFATc1), a key regulator of osteoclast differentiation, is activated and regulates several osteoclast-specific genes such as TRAP, cathepsin K, and DC-STAMP.[5].

Salicornia europaea L. (SE), also known as *Salicornia herbacea* L., is an annual halophyte that grows in salt marshes, belongs to the Amaranthaceae family, and is distributed in the west coast of the Korean peninsula. Its common name is glasswort, and it is commonly called hamcho in Korea. This plant has been traditionally used in salads, fermented foods, and other dishes [6]. It is also employed as a folk medicine to treat various diseases such as headaches and scurvy[7]. Additionally, in our country, it has been commercially available as a health supplement. Recently studies have suggested that SE has health-benefitting properties via the exertion of antioxidant, anti-inflammatory, anti-neuroinflammatory, anti-amnesic, anti-diabetic, and anti-hyperlipidemic effects[8-10]. Moreover, SE has been considered to potentially have of anti-osteoporotic effects based on its ability to inhibit adipogenesis and promote osteoblast differentiation [11]. Since SE grows under high-salt conditions, it contains abundant bioactive phytochemicals, such as flavonoids and saponins, to overcome salt stress[9,12]. Dicafeoylquinic acids (DCQAs) and two flavonoid glycosides (isorhamnetin 3-O- β -D-glucoside and quercetin 3-O- β -D-glucoside) isolated from SE have potential as anti-metastatic and anti-cancer agents that inhibit MMP9 and/or MMP2 activity in fibrosarcoma HT-1080 cells [13]. However, to the best of our knowledge, studies on the osteoclast inhibitory mechanism and the anti-osteoporotic effect of SE and its constituents have not been reported to date. In this study, we investigated the inhibitory effect of water extract of desalted SE (WSE) on RANKL-induced osteoclast differentiation and bone loss in ovariectomized (OVX) mice. The inhibitory effects of its DCQA fraction were also investigated.

2. Materials and Methods

2.1. Sample Preparation and Isolation of Three DCQAs

Dried aerial parts of SE were obtained from Dasarang Co., Ltd., in Shinan County, South Korea. Ground samples (1.3 kg) were soaked in 52 L of distilled water at room temperature for 1 h. After draining, the residues were extracted with hot water (19.5 L) at 95°C for 5 h. The hot water extracts were filtered through a 140-mesh filter (Whatman, Maidstone, England) and concentrated at 60°C under vacuum conditions to reach 15 °Brix of solid content. These concentrates were spray-dried at operating conditions including inlet air temperature (190°C) and outlet air temperature (60°C) to obtain WSE. Three DCQAs were purified and isolated from the WSE using ODS column chromatography and identified by MS and NMR analyses (supplementary method). The MS and NMR spectroscopic data are also shown in the supplementary tables and figures.

2.2. Osteoclast Differentiation

Bone marrow cells were isolated from the femurs of 8-week-old male mice (Koatech, Pyeongtaek, Gyeonggi-do, South Korea) and cultured in 10% FBS, α -MEM containing 1% FBS (Gibco, Grand Island, NY, USA). Cultured. Penicillin/streptomycin and recombinant M-CSF (25 ng/ml; Miltenyi Biotec, Bergisch Gladbach, Germany) are placed in a 5% CO incubator at 37 °C. After 3 days, BMDMs were seeded and incubated in the presence of recombinant RANKL (100 ng/ml; Peprotech, Cranbury, NJ) for 3 days with daily medium changes.

2.3. TRAP Staining

Osteoclast formation was assessed using a TRAP staining kit (Kamiya Biomedical Company, Tukwila, WA, USA) according to the manufacturer's instructions. The quantity of TRAP-positive cells possessing three or more nuclei was determined through examination under a light microscope.

2.4. F-Actin Ring Formation Staining

BMDMs were plated on cover glass and induced to differentiate into osteoclasts. Following this, the cells were fixed using 4% formaldehyde and permeabilized using 0.1% Triton X-100 (Sigma-Aldrich, St. Louis, MO, USA). They were then stained with Alexa Fluor 594-phalloidin (Invitrogen, Carlsbad, CA, USA) for 2 hours. Subsequently, the cells were mounted onto slides, and the nuclei were counterstained with 4',6-diamidino-2-phenylindole (Invitrogen). Images were observed using a fluorescence microscope.

2.5. Bone Resorption Assay

BMDMs were cultured on an Osteo Assay Surface multiple-well plate (Corning Costar, Corning, NY, USA). After 7 days, the RANKL-stimulated BMDMs were cultured with 20% SDS for 10 min to remove the cells. The areas absorbed onto the discs were examined using a microscope and quantified using ImageJ software (National Institutes of Health, Bethesda, MD, USA).

2.6. Real-Time Quantitative PCR (qPCR)

Total RNA was isolated from cells using an Easy-BLU Total RNA Extraction Kit (Intron Biotechnology, Seongnam, Gyeonggi-do, Korea), and cDNA was generated using ReverTra Ace qPCR RT Master Mix (TOYOBO Bio-Technology, Osaka, Japan), according to the manufacturer's instructions. The primers used for qPCR are shown in Table 1. Target gene expression levels were performed using QGreen 2× SybrGreen qPCR Master Mix and a CFX Connect Real-time PCR Detection System (Bio-Rad, Hercules, CA, USA).

Table 1. Primer sequences used in this study.

Genes	Sequence 5'-3'
TRAP	F: CTGGAGTGCACGATGCCAGCGACA R: TCCGTGCTCGGCGATGGACCAGA
DC-STAMP	F: CCAAGGAGTCGTCCATGATT R: GGCTGCTTTGATCGTTTCTC
NFATc1	F: CTCGA AAGACAGTGGAGCAT R: CGGCTGCCTTCC GTTCATAG
Cathepsin K	F: GGCCAACTCAAGAAGA AAAC R: GTGCTTGCTTCCCTTCTGG
β -actin	F: AGGCCAGAGCAAGAGAG R: TCAACATGATC TGGGTCATC

2.7. Western Blot

Cells were lysed in lysis buffer supplemented with protease inhibitor (Roche, Mannheim, Germany) and phosphatase inhibitor (Sigma-Aldrich, St. Louis, MO, USA). Blots were then probed with primary antibodies against, $\text{I}\kappa\text{B-}\alpha$, phospho-form of p65, JNK, p38, and ERK (Cell Signaling Technology, Beverly, MA, USA), and β -actin (Santa Cruz Biotechnology, Dallas, TX, USA). The secondary antibodies used were HRP-labelled anti-rabbit or anti-mouse antibodies. The proteins were detected using Clarity Western ECL Substrate (Bio-Rad), and densities were quantified using ImageJ.

2.8. Intracellular ROS Detection

BMDMs were stimulated with RANKL, with or without compounds for 24 h. Cells were washed and then incubated with 2', 7'-dichlorofluorescein diacetate (Sigma-Aldrich) for 30 min at 37°C. Oxidative conversion was detected using a fluorescence microscope.

2.9. Animal Experiments

Seven-week-old C57BL/6 female mice were purchased from Koatech. OVX mice were divided into five groups—a sham group and four OVX groups—and treated either with PBS (vehicle control) or WSE (40, 80, 160 mg/kg) by gavage six times per week for 12 weeks. All mice were sacrificed, and the femurs were used for micro-computed tomography (μ CT). All in vivo animal studies were approved by the Institutional Animal Care and Use Committee of Chonnam National University (Approval No. 2021-111)

2.10. μ CT Analysis

The femurs were analyzed using high-resolution μ CT (Sky-Scan 1172TM, Skyscan, Kontich, Belgium). To determine the femoral morphometry, bone alterations were quantified by analyzing bone mineral density (BMD), bone volume per tissue volume (BV/TV), trabecular thickness (Tb.Th), trabecular spacing (Tb.Sp), and trabecular number (Tb.N) using data analysis software (CTAn).

2.11. Statistical Analysis

The statistical significance of the intergroup differences was determined using one-way analysis of variance (ANOVA), followed by Tukey's post hoc test or the two-tailed Student's t-test. All statistical analyses were performed using GraphPad Prism 8 (GraphPad Software, San Diego, CA, USA). A p-value < 0.05 was considered statistically significant.

3. Result

3.1. WSE Inhibited RANKL-Induced Osteoclast Differentiation and Bone Resorption

The formation of TRAP-positive cells was completely inhibited by WSE at a dose of 5 μ g/ml (Figure. 1A and 1B). WSE also showed that the area percentage of absorption pits decreased in a dose-dependent manner (Figure. 1C and 1D). Osteoclasts form F-actin rings to reorganize the actin cytoskeleton and form resorption cavities on the bone surface [14]. We therefore investigated how WSE affects F-actin ring formation. WSE treatment inhibited F-actin ring formation caused by RANKL (Figure. 1E). These results suggest that WSE exerts an inhibitory effect on osteoclast differentiation and bone resorption induced by RANKL.

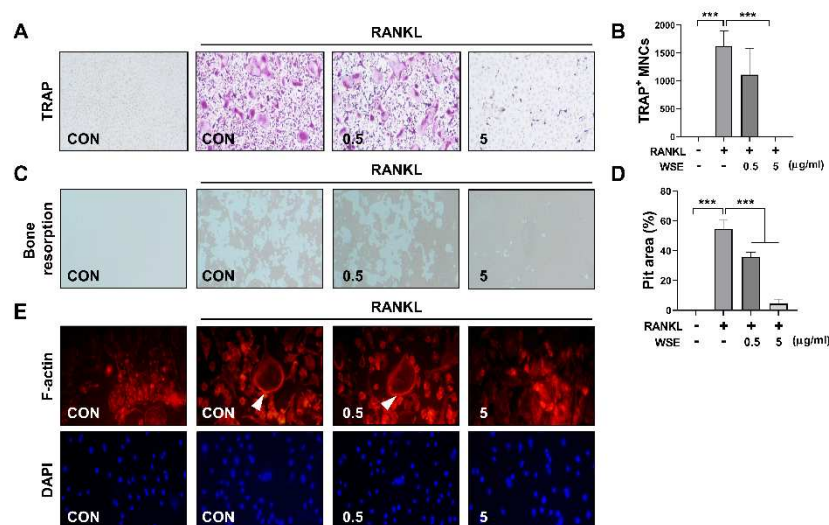


Figure 1. WSE suppressed RANKL-induced osteoclast differentiation. BMDMs were pretreated with WSE (0.5 and 5 μ g/ml) for 2 h and subsequently stimulated with RANKL for 3 days. RANKL-induced osteoclasts were fixed and stained to detect TRAP activity (A). TRAP-positive cells were counted (B). Representative images of bone resorption pits were observed (C), and resorption pits were quantified

using ImageJ software (D). RANKL-induced F-actin rings were stained with Alexa Fluor 594-phalloidin and visualized (E). Results are presented as mean \pm SD. ***P < 0.001. 3.1. Subsection.

3.2. WSE Suppressed Gene Expression Related to RANKL-Induced Osteoclastogenesis in BMDMs

NFATc1 is expressed at intermediate or late stages of osteoclast differentiation and regulates the transcription of osteoclast-specific genes [5]. To support the inhibitory effect of WSE on osteoclast differentiation induced by RANKL, we further analyzed the expression of osteoclast specific genes via qPCR. RANKL strongly upregulated the gene expression of NFATc1, TRAP, cathepsin K and DC-STAMP, which was suppressed by WSE treatment in a dose-dependent manner (Figure. 2A-2D).

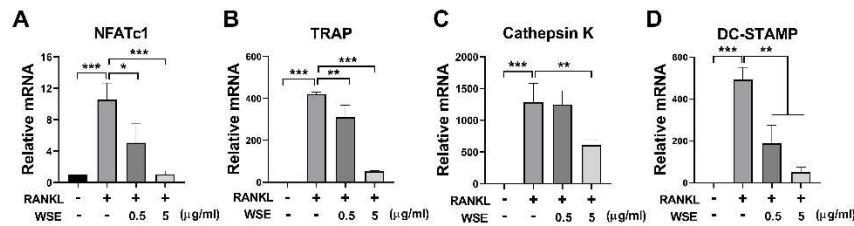


Figure 2. WSE inhibited RANKL-induced osteoclast-specific gene expression. The mRNA expression levels of NFATc1 (A), TRAP (B), Cathepsin K (C), and DC-STAMP (D) were quantified by qPCR. β -actin was used as the internal control. Results are presented as mean \pm SD. *P < 0.05, **P < 0.01, ***P < 0.001.

3.3. Oral Administration of WSE Attenuated OVX-Induced Bone Loss in Mice

We further investigated whether WSE administration attenuated bone loss in OVX mice. The body weight of OVX mice was increased compared to sham controls; however, upon administration of WSE, body weight significantly decreased in a dose-dependent manner. (Figure. S1A-S1C). Additionally, the increase in abdominal fat associated with OVX surgery was also significantly reduced in the group receiving 160 mg/kg WSE compared to OVX controls (Figure S1E). Quantitative morphological analysis showed that OVX had significantly reduced BMD compared to the sham group (Figure. 3A and 3B). These changes were partially ameliorated by oral administration of WSE in a dose-dependent manner (Figure. 3A and 3B). BV/TV and Tb.N, which were decreased by OVX, were increased by WSE administration, whereas Tb.Th and Tb.Sp were not restored to baseline (Figure. 3C-3F). These results imply that oral administration of WSE may prevent bone loss in postmenopausal women.

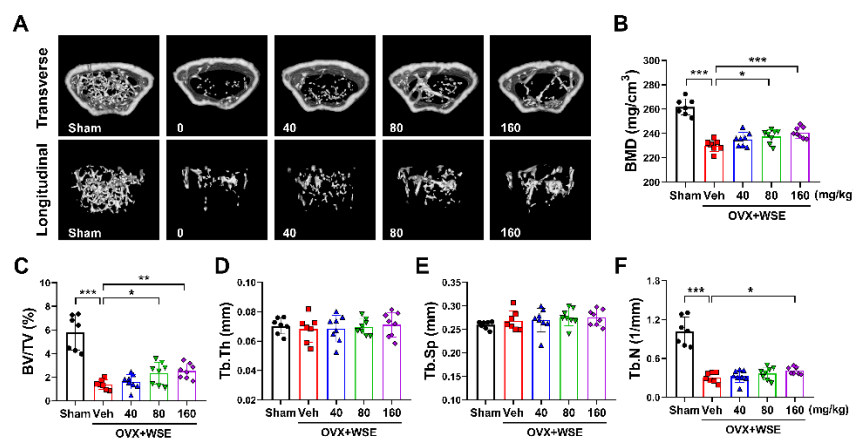


Figure 3. WSE prevented OVX-induced bone loss in mice. Representative μ CT images of mouse femurs (A). Analyses of BMD (B), BV/TV (C), Tb.Th (D), Tb.Sp (E), and Tb.N (F) were conducted using μ CT. Results are presented as mean \pm SD. * $P < 0.05$, ** $P < 0.01$, *** $P < 0.001$.

3.4. Identification of Three DCQAs in WSE

We performed analyses via UPLC-ESI-Q-TOF MS with WSE samples to obtain a metabolite profile. Thirty-three compounds, including DCQAs, flavonoids, and triterpene glycosides, were detected on the ion chromatograms (Figure. S2 and Table S1) [15-17]. DCQAs and triterpene glycosides among them were considered the main compounds in WSE. To determine accurate metabolite structures, we attempted to purify and isolate compounds from the WSE. Three DCQAs were successfully isolated, as white amorphous powder, from the WSE sample by ODS column chromatography. The high purities (>95%) of the three isolated DCQAs were confirmed by their MS and ^1H NMR spectra (Figure. S3-S7, S11, S12, S16, S17), and they were confirmed to have the same molecular weight (516) and molecular formula ($\text{C}_{25}\text{H}_{24}\text{O}_{12}$) in the HR-ESI-MS data (Table S2). The MS results were supported by their ^{13}C NMR spectra, which contained a total of 25 carbon signals, including three carbonyl carbons at δ 178.6-169.6 and one oxygenated quaternary carbon of quinic acid at δ 71.5-75.4 (C-1) (Table S4). Also, the ^1H NMR spectra of the three DCQAs confirmed the presence of DCQA corresponding to proton signals of two caffeic acids at δ 6.26-7.62 (H-2'-H-8' and H-2''-H-8'') and one quinic acid at δ 2.13-5.67 (H-2-H-6) (Table S3). However, the chemical shifts of three oxygenated proton signals at δ 4.32-5.67 in quinic acid significantly differed among the three DCQAs. Connections between caffeic acid and quinic acid were confirmed by the 2D-NMR experiments, including ^1H - ^1H COSY, HSQC, and HMBC (Figure. S8-S10, S13-S15, and S18-S20). Finally, the three DCQAs were identified as 3,4-DCQA, 3,5-DCQA, and 4,5-DCQA by comparison with previously reported MS and NMR results (Figure. 4A-C) [15,16,18].

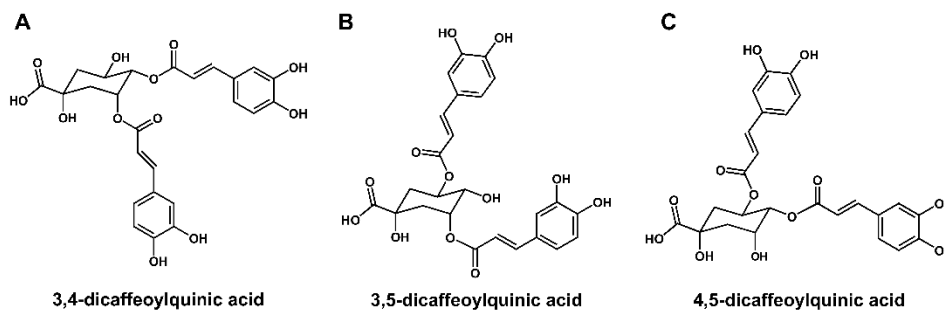


Figure 4. Structure of three DCQAs isolated from WSE. Structures of 3,4-DCQA (A), 3,5-DCQA (B), and 4,5-DCQA (C) isolated from WSE.

3.5. DCQAs Extracted from WSE Inhibited RANKL-Induced Osteoclast Differentiation

Previous studies have shown that 3,5-DCQA isolated from *Chrysanthemum zawadskii* var. *latilobum* exerts an inhibitory effect on RANKL-induced osteoclastogenesis [19]. Therefore, we sought to determine whether a fraction containing DCQAs and chemical compounds isolated from the fraction possess anti-osteoclastogenic properties. TRAP-positive cells were eliminated after treatment with DCQAs at a dose of 100 $\mu\text{g}/\text{ml}$ (Figure. 5A and 5B). Bone resorption induced by RANKL was also suppressed by DCQA fraction treatment in a dose-dependent manner (Figure. 5A and 5C). Moreover, DCQA fraction treatment reduced F-actin ring formation by RANKL in a dose-dependent manner (Figure. 5D). We further investigated the inhibitory effect of single compounds contained in the fraction. The three DCQAs reduced the number of TRAP-positive cells and the size of the pit area formed by RANKL (Figure. S21A and S21B, Figure. 5E and 5F).

Next, we investigated the effect of DCQA on mRNA expression of osteoclast-specific genes. As expected, fractions containing DCQAs inhibited RANKL-induced expression of all genes tested in a dose-dependent manner (Figure. 6A). The three DCQAs also effectively inhibited the expression of the corresponding genes, with 4,5-DCQA showing the highest inhibitory ability. We also examined whether the DCQA-containing fraction influences RANKL-induced activation of NF- κ B and MAPKs. We also investigated whether the DCQA-containing fractions affected NF- κ B and MAPK activation induced by RANKL. Western blot analysis showed that RANKL treatment enhanced the activation of NF- κ B and MAPKs, including ERK, p38 and JNK (Figure. 6C and 6D). Phosphorylation of p65, ERK, p38 and degradation of I κ B- α were effectively inhibited by DCQA fraction treatment, although JNK phosphorylation was not affected (Figure 6C and 6D). These findings suggest that DCQAs may be the essential compounds of WSE associated with the inhibition of osteoclast differentiation.

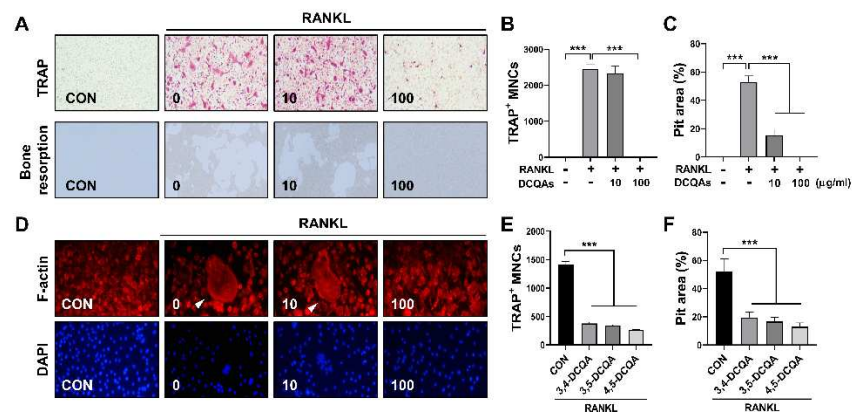


Figure 5. Three DCQA derivatives from WSE suppressed RANKL-induced osteoclast differentiation. BMDMs were pretreated with DCQA fractions (10 and 100 μ g/ml) for 2 h and subsequently stimulated with RANKL for 3 days. Osteoclast differentiation and osteoclastic bone resorption induced by RANKL were imaged (A). TRAP-positive cells were counted (B). Quantification of the resorption pits was performed using ImageJ software (C). RANKL-induced F-actin rings were stained with Alexa Fluor 594-phalloidin and imaged (D). BMDMs were pretreated with three types of DCQAs (10 μ M) for 2 h and subsequently stimulated with RANKL for 3 days. TRAP-positive cells were counted (E). Osteoclastic bone resorption function was quantified using ImageJ software (F). Results are presented as mean \pm SD. *** $P < 0.001$.

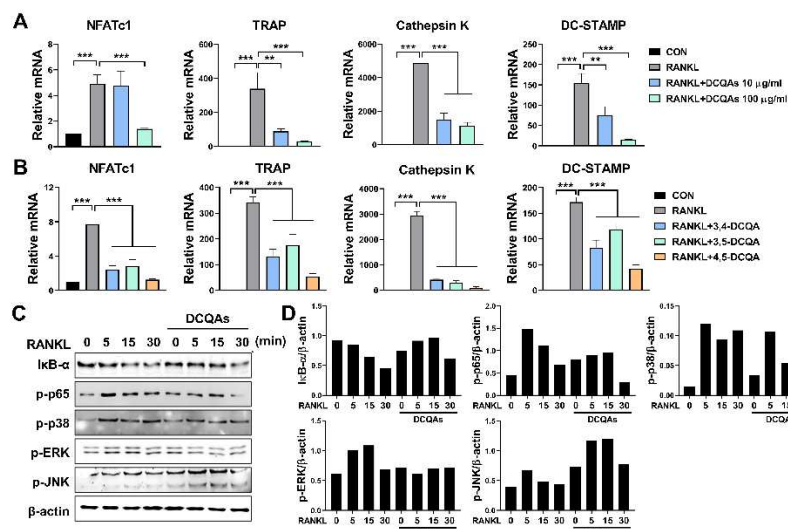


Figure 6. Three DCQA derivatives from WSE regulated RANKL-induced osteoclastogenesis via osteoclast-specific gene expression and activation of NF- κ B and MAPKs. BMDMs were pretreated with DCQA fractions (10 and 100 μ g/ml) and three constituent DCQAs (10 μ M) for 2 h and subsequently stimulated with RANKL for 3 days. Regulation of gene expression levels of NFATc1, TRAP, cathepsin K, and DC-STAMP by the DCQA fractions (A) and the three constituent DCQAs (B) was determined using qPCR. β -actin was used as the internal control. Western blotting was used to analyze the expression of I κ B- α degradation, as well as the phosphorylation of p65, p38, ERK, and JNK in RANKL-stimulated BMDMs (C). Antibody against β -actin was used to confirm the loading doses. Quantification analyses of protein levels were performed using ImageJ software (D). Results are presented as mean \pm SD. **P < 0.01, ***P < 0.001.

3.6. WSE and DCQAs reduced ROS production induced by RANKL

ROS are known to promote osteoclast differentiation and to be involved in the early stages of osteoclast activation. RANKL-induced intracellular ROS production is considered an upstream component regulating osteoclast differentiation and activation [20,21]. Accordingly, we finally investigated whether WSE and DCQAs affect RANKL-induced intracellular ROS production. WSE dose-dependently suppressed the ROS production induced by RANKL and almost completely inhibited it at a dose of 5 μ g/ml (Figure. 7A and 7B). The number of ROS-positive cells was also reduced by DCQA fraction treatment in a dose-dependent manner (Figure. 7C and 7D). All three compounds tested also exerted inhibitory effects on RANKL-induced ROS formation (Figure. 7E and 7F). These results suggest that WSE and DCQAs may inhibit RANKL-induced osteoclast differentiation by scavenging ROS.

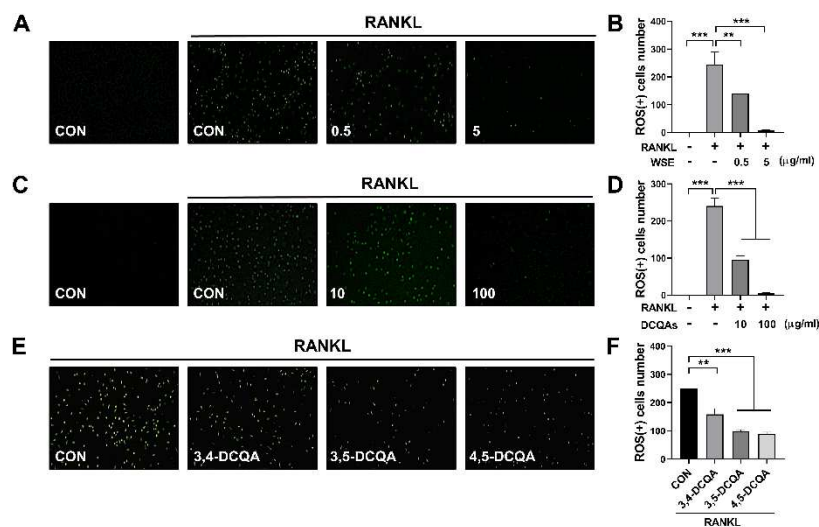


Figure 7. WSE and its compounds suppressed RANKL-induced ROS production. BMDMs were pretreated with WSE (0.5 and 5 μ g/ml), DCQA fractions (10 and 100 μ g/ml), and three constituent DCQAs (10 μ M) for 2 h and subsequently stimulated with RANKL. After 24 h, cells were incubated with DCFDA (2', 7'-dichlorofluorescein diacetate) and detected using fluorescence microscopy (A, C, and E). The number of ROS-positive cells was counted in each well (B, D, and F). Results are presented as mean \pm SD. **P < 0.01, ***P < 0.001.

4. Discussion

Bone homeostasis is maintained by the balance of osteoclast and osteoblast. The imbalance can be disrupted by various processes and conditions, such as menopause, aging, and chronic inflammation [1,22]. Such disruptions lead to bone-related diseases including osteoporosis. In postmenopausal women, osteoporosis is caused by accelerated osteoclast differentiation due to estrogen deficiency [2]. Many studies have found that excessive differentiation and activity of osteoclasts is mainly associated with bone loss and causes the progression of metabolic bone diseases

[23]. Therefore, inhibiting the differentiation and activation of osteoclasts is considered the most efficient way to prevent and treat osteoporosis.

SE and its bioactive constituents are known to have various health-promoting properties [9,12]. SE extract inhibited adipogenesis and promoted osteoblastogenesis in an in vitro study using 3T3-L1 pre-adipocytes and MC3T3-E1 pre-osteoblasts [11], suggesting that the SE extract can be developed as a new preventive or therapeutic agent for osteoporosis, as elevated adipogenesis in bone and a lack of osteoblastogenesis results in osteoporosis and bone loss. In the present study, we observed that WSE suppressed osteoclast differentiation and bone resorption activity. Additionally, WSE treatment dose-dependently reduced the mRNA expression of osteoclastogenesis-related genes upregulated by RANKL. In an in vivo study using OVX mice, oral administration of WSE improved BMD, BV/TV, and Tb.N. These results indicate that WSE administration may improve bone loss due to estrogen deficiency by suppressing osteoclastogenesis.

SE contains various bioactive constituents such as caffeoylquinic acids, flavonoids, triterpenoid saponins, and pentadecylferulate. These compounds are involved in bone remodeling via the promotion of osteoblastogenesis or the suppression of adipogenesis and osteoclastogenesis [12,13,17,24,25]. In the present study, we analyzed the metabolite profile of WSE and found DCQAs and triterpene glycosides as the main compounds in WSE. Additionally, we isolated three types of DCQAs and identified them as 3,4-, 3,5-, and 4,5-DCQA by comparison with previous MS and NMR results [15,16,18]. Treatment with a fraction containing DCQAs, as well as with the three constituent DCQAs, suppressed RANKL-induced osteoclast differentiation and osteoclastic bone resorption. Additionally, RANKL-induced expression of osteoclastogenesis-related genes was also reduced by treatment with the fraction containing DCQAs, as well as with the three constituent DCQAs, suggesting that DCQAs may be the main components of WSE that inhibit osteoclastogenesis.

Binding of RANKL to RANK receptor leads to the recruitment of TRAF6 and subsequently activates NF- κ B and MAPKs responsible for osteoclast differentiation and activation. Both NF- κ B and MAPKs can control the expression of NFATc1, a master transcriptional regulator of osteoclast differentiation-related genes [4,5]. In this study, DCQA fraction treatment suppressed the activation of NF- κ B, p38, and ERK MAPKs. It is likely that bioactive components, including DCQAs in WSE, regulate upstream signaling (e.g., TRAF6) of NF- κ B and MAPKs in osteoclast precursors. Additionally, ROS can be produced by RANKL in osteoclast precursors through TRAF6-mediated pathways and mediate RANKL-induced osteoclastogenesis by regulating NF- κ B and MAPKs activation [21]. In the present study, a DCQA-containing fraction, three constituent DCQA compounds, and WSE inhibited RANKL-induced ROS production. SE is known to contain various anti-oxidative compounds, including tungtungmadic acid, quercetin, chlorogenic acid, and caffeoylquinic acid [12,15] reported that four new DCQA derivatives isolated from SE exert anti-oxidative activity. Taken together, these results show that WSE and its bioactive DCQAs may inhibit RANKL-induced osteoclast differentiation by suppressing RANKL-induced ROS production.

5. Conclusions

In conclusion, our results revealed that WSE suppresses the differentiation of osteoclasts and its oral administration attenuates bone loss in OVX mice. Moreover, DCQAs are the main active compounds in WSE that exert anti-osteoclastogenic activity by regulating RANKL-induced activation of NF- κ B and MAPKs to inhibit ROS production. These results suggest that SE or its active constituents can be developed as preventive or therapeutic agents against osteoporosis. Further studies are needed to prove the safety of WSE ingestion by analyzing the concentrations of heavy metals, such as arsenic and mercury, and performing non-clinical research.

Supplementary Materials: The following supporting information can be downloaded at: www.mdpi.com/xxx/s1, Figure S1: Effect of ovariectomy and WSE on body weight and organ weight; Figure S2: UPLC-ESI-Q-TOF MS (negative) TIC chromatogram of WSE.; Figure S3: Ion chromatogram and ESI-MS spectrum of 3,4-dicaffeoylquinic acid; Figure S4: Ion chromatogram and ESI-MS spectrum of 3,5-dicaffeoylquinic acid; Figure S5: Ion chromatogram and ESI-MS spectrum of 4,5-dicaffeoylquinic acid; Figure S6: 1H NMR (500 MHz, CD₃OD) spectrum of 3,4-dicaffeoylquinic acid; Figure S7: 13C NMR (125 MHz, CD₃OD) spectrum of 3,4-

dicafeoylquinic acid; Figure S8: 1H-1H COSY spectrum of 3,4-dicafeoylquinic acid; Figure S9: HSQC spectrum of 3,4-dicafeoylquinic acid; Figure S10: HMBC spectrum of 3,4-dicafeoylquinic acid; Figure S11: 1H NMR (500 MHz, CD3OD) spectrum of 3,5-dicafeoylquinic acid; Figure S12: 13C NMR (125 MHz, CD3OD) spectrum of 3,5-dicafeoylquinic acid; Figure S13: 1H-1H COSY spectrum of 3,5-dicafeoylquinic acid; Figure S14: HSQC spectrum of 3,5-dicafeoylquinic acid; Figure S15: HMBC spectrum of 3,5-dicafeoylquinic acid; Figure S16: 1H NMR (500 MHz, CD3OD) spectrum of 4,5-dicafeoylquinic acid; Figure S17: 13C NMR (125 MHz, CD3OD) spectrum of 4,5-dicafeoylquinic acid; Figure S18: 1H-1H COSY spectrum of 4,5-dicafeoylquinic acid; Figure S19: HSQC spectrum 4,5-dicafeoylquinic acid; Figure S20: HMBC spectrum of 4,5-dicafeoylquinic acid; Figure S21: Three DCQA derivatives from WSE suppressed RANKL-induced osteoclast differentiation; Table S1: LC-ESI-MS data of WSE; Table S2: HR-ESI-MS (negative) data of three dicafeoylquinic acids isolated from a water extract of desalted *Salicornia europaea*; Table S3: 1H NMR (500 MHz) data of three dicafeoylquinic acids (isolated from a water extract of desalted *Salicornia europaea*) in CD3OD; Table S4: 13C NMR (125 MHz) data of three dicafeoylquinic acids (isolated from a water extract of desalted *Salicornia europaea*) in CD3OD .

Author Contributions: Conceptualization, J.-Y.C. and J.-H.P.; methodology, A.-R.J. and Y.-J.L.; software, D.-Y.K. and T.-S.L.; validation, D.-H.J. and Y.-J.K. and I.-S.S.; formal analysis, J.-H.A. and E.-J.S.; investigation, J.S.O. and A.L. and S.H.S.; resources, H.-S.K. and M.-J.K.; data curation, Y.J.S.; writing—original draft preparation, A.-R.J. and Y.-J.L.; writing—review and editing, Y.-J.L. and J.-H.P.; visualization, Y.-J.L.; supervision, J.-H.P.; project administration, J.-H.P.; funding acquisition, J.-H.P.

Funding: This research was funded by Commercialization's Promotion Agency for R&D Outcomes grant (Grant No. 2023C200) funded by Korean government (MSIT).

Institutional Review Board Statement: The animal study protocol was approved by the Institutional Animal Care and Use Committee of Chonnam National University (approval number: CNU IACUC-YB-2021-111).

Data Availability Statement: The data that support the finding of this study are available from the corresponding author upon reasonable request.

Conflicts of Interest: The authors have no competing interests to declare that are relevant to the content of this article.

References

- Feng, X.; McDonald, J.M. Disorders of bone remodeling. *Annu Rev Pathol* **2011**, *6*, 121-145, doi:10.1146/annurev-pathol-011110-130203.
- Eastell, R.; O'Neill, T.W.; Hofbauer, L.C.; Langdahl, B.; Reid, I.R.; Gold, D.T.; Cummings, S.R. Postmenopausal osteoporosis. *Nat Rev Dis Primers* **2016**, *2*, 16069, doi:10.1038/nrdp.2016.69.
- Riggs, B.L. The mechanisms of estrogen regulation of bone resorption. *J Clin Invest* **2000**, *106*, 1203-1204, doi:10.1172/jci11468.
- Amarasekara, D.S.; Yun, H.; Kim, S.; Lee, N.; Kim, H.; Rho, J. Regulation of Osteoclast Differentiation by Cytokine Networks. *Immune Netw* **2018**, *18*.
- Park, J.H.; Lee, N.K.; Lee, S.Y. Current Understanding of RANK Signaling in Osteoclast Differentiation and Maturation. *Mol Cells* **2017**, *40*, 706-713, doi:10.14348/molcells.2017.0225.
- Patel, S. *Salicornia*: evaluating the halophytic extremophile as a food and a pharmaceutical candidate. *3 Biotech* **2016**, *6*, 104, doi:10.1007/s13205-016-0418-6.
- Isca, V.; Seca, A.; Pinto, D.; Silva, A. An overview of *Salicornia* genus: The phytochemical and pharmacological profile. 2014; Volume 2, pp. 145-176.
- Ha, B.J.; Lee, S.H.; Kim, H.J.; Lee, J.Y. The role of *Salicornia* herbacea in ovariectomy-induced oxidative stress. *Biol Pharm Bull* **2006**, *29*, 1305-1309, doi:10.1248/bpb.29.1305.
- Karthivashan, G.; Park, S.Y.; Kweon, M.H.; Kim, J.; Haque, M.E.; Cho, D.Y.; Kim, I.S.; Cho, E.A.; Ganesan, P.; Choi, D.K. Ameliorative potential of desalted *Salicornia europaea* L. extract in multifaceted Alzheimer's-like scopolamine-induced amnesic mice model. *Sci Rep* **2018**, *8*, 7174, doi:10.1038/s41598-018-25381-0.
- Park, S.H.; Ko, S.K.; Choi, J.G.; Chung, S.H. *Salicornia* herbacea prevents high fat diet-induced hyperglycemia and hyperlipidemia in ICR mice. *Arch Pharm Res* **2006**, *29*, 256-264, doi:10.1007/bf02969402.
- Karadeniz, F.; Kim, J.-A.; Ahn, B.-N.; Kwon, M.S.; Kong, C.-S. Effect of *Salicornia* herbacea on Osteoblastogenesis and Adipogenesis in Vitro. *Marine Drugs* **2014**, *12*, 5132-5147.
- Giordano, R.; Saii, Z.; Fredsgaard, M.; Hulkko, L.S.S.; Poulsen, T.B.G.; Thomsen, M.E.; Henneberg, N.; Zucolotto, S.M.; Arendt-Nielsen, L.; Papenbrock, J.; et al. Pharmacological Insights into Halophyte Bioactive Extract Action on Anti-Inflammatory, Pain Relief and Antibiotics-Type Mechanisms. *Molecules* **2021**, *26*, 3140.
- Hwang, Y.P.; Yun, H.J.; Choi, J.H.; Chun, H.K.; Chung, Y.C.; Kim, S.K.; Kim, B.H.; Kwon, K.I.; Jeong, T.C.; Lee, K.Y.; et al. 3-Caffeoyl, 4-dihydrocaffeoylquinic acid from *Salicornia* herbacea inhibits tumor cell

- invasion by regulating protein kinase C-delta-dependent matrix metalloproteinase-9 expression. *Toxicol Lett* **2010**, *198*, 200-209, doi:10.1016/j.toxlet.2010.06.018.
14. Wang, Q.; Xie, Y.; Du, Q.S.; Wu, X.J.; Feng, X.; Mei, L.; McDonald, J.M.; Xiong, W.C. Regulation of the formation of osteoclastic actin rings by proline-rich tyrosine kinase 2 interacting with gelsolin. *J Cell Biol* **2003**, *160*, 565-575, doi:10.1083/jcb.200207036.
 15. Cho, J.Y.; Kim, J.Y.; Lee, Y.G.; Lee, H.J.; Shim, H.J.; Lee, J.H.; Kim, S.J.; Ham, K.S.; Moon, J.H. Four New Dicafeoylquinic Acid Derivatives from Glasswort (*Salicornia herbacea* L.) and Their Antioxidative Activity. *Molecules* **2016**, *21*, doi:10.3390/molecules21081097.
 16. Kim, J.; Cho, J.-Y.; Ma, Y.-K.; Park, K.; Lee, S.-H.; Ham, K.-S.; Lee, H.; Park, K.-H.; Moon, J.-H. Dicafeoylquinic acid derivatives and flavonoid glucosides from glasswort (*Salicornia herbacea* L.) and their antioxidative activity. *Food Chemistry - FOOD CHEM* **2011**, *125*, 55-62, doi:10.1016/j.foodchem.2010.08.035.
 17. Kim, Y.A.; Kong, C.S.; Lee, J.I.; Kim, H.; Park, H.Y.; Lee, H.S.; Lee, C.; Seo, Y. Evaluation of novel antioxidant triterpenoid saponins from the halophyte *Salicornia herbacea*. *Bioorg Med Chem Lett* **2012**, *22*, 4318-4322, doi:10.1016/j.bmcl.2012.05.017.
 18. Ge, L.; Wan, H.; Tang, S.; Chen, H.; Li, J.; Zhang, K.; Zhou, B.; Fei, J.; Wu, S.; Zeng, X. Novel caffeoylquinic acid derivatives from *Lonicera japonica* Thunb. flower buds exert pronounced anti-HBV activities. *RSC Adv* **2018**, *8*, 35374-35385, doi:10.1039/c8ra07549b.
 19. Kim, A.R.; Kim, H.S.; Kim, D.K.; Lee, J.H.; Yoo, Y.H.; Kim, J.Y.; Park, S.K.; Nam, S.T.; Kim, H.W.; Park, Y.H.; et al. The Extract of *Chrysanthemum zawadskii* var. *latilobum* Ameliorates Collagen-Induced Arthritis in Mice. *Evidence-Based Complementary and Alternative Medicine* **2016**, *2016*, 3915013, doi:10.1155/2016/3915013.
 20. Ha, H.; Kwak, H.B.; Lee, S.W.; Jin, H.M.; Kim, H.M.; Kim, H.H.; Lee, Z.H. Reactive oxygen species mediate RANK signaling in osteoclasts. *Exp Cell Res* **2004**, *301*, 119-127, doi:10.1016/j.yexcr.2004.07.035.
 21. Lee, N.K.; Choi, Y.G.; Baik, J.Y.; Han, S.Y.; Jeong, D.-w.; Bae, Y.S.; Kim, N.; Lee, S.Y. A crucial role for reactive oxygen species in RANKL-induced osteoclast differentiation. *Blood* **2005**, *106*, 852-859, doi:10.1182/blood-2004-09-3662.
 22. Meirou, Y.; Jovanovic, M.; Zur, Y.; Habib, J.; Colombo, D.F.; Twaik, N.; Ashkenazi-Preiser, H.; Ben-Meir, K.; Mikula, I.; Reuven, O.; et al. Specific inflammatory osteoclast precursors induced during chronic inflammation give rise to highly active osteoclasts associated with inflammatory bone loss. *Bone Research* **2022**, *10*, 36, doi:10.1038/s41413-022-00206-z.
 23. Teitelbaum, S.L. Bone resorption by osteoclasts. *Science* **2000**, *289*, 1504-1508, doi:10.1126/science.289.5484.1504.
 24. Wang, X.; Zhang, M.; Zhao, Y.; Wang, H.; Liu, T.; Xin, Z. Pentadecyl ferulate, a potent antioxidant and antiproliferative agent from the halophyte *Salicornia herbacea*. *Food Chem* **2013**, *141*, 2066-2074, doi:10.1016/j.foodchem.2013.05.043.
 25. Ramesh, P.; Jagadeesan, R.; Sekaran, S.; Dhanasekaran, A.; Vimalraj, S. Flavonoids: Classification, Function, and Molecular Mechanisms Involved in Bone Remodelling. *Frontiers in Endocrinology* **2021**, *12*, doi:10.3389/fendo.2021.779638.

Disclaimer/Publisher's Note: The statements, opinions and data contained in all publications are solely those of the individual author(s) and contributor(s) and not of MDPI and/or the editor(s). MDPI and/or the editor(s) disclaim responsibility for any injury to people or property resulting from any ideas, methods, instructions or products referred to in the content.